

Supporting Information

Management of Locally Excited States for Purine-based TADF Emitters: A Method to Reduce Device Efficiency Roll-Off

Yangbo Wu, Yuming Zhang, Chunhao Ran, Jingbo Lan, Zhengyang Bin, Jingsong You*

Key Laboratory of Green Chemistry and Technology of Ministry of Education,
College of Chemistry, Sichuan University, 29 Wangjiang Road, Chengdu 610064, P.R. China

*E-mail: binzhengyang@scu.edu.cn

Table of Contents

I. General Remarks	S1
II. OLED Fabrication and Characterization	S2
III. Theoretical Calculation	S2
IV. Synthesis and Characterization	S3
V. Crystal Data	S9
VI. Additional Spectra and Data	S13
VII. References	S19
VIII. Copies of NMR Spectra	S20
IX. Copies of High-Resolution Mass Spectra	S28

I. General Remarks

All commercially available reagents and chemicals were used as received without further purification. Unless otherwise noted, all reactions were carried out using Schlenk techniques under a nitrogen atmosphere. The heat source for all heating reactions is an oil bath. The solvents were dried and purified using an Innovative Technology PS-MD-5 Solvent Purification System. NMR spectra were obtained on an Agilent 400-MR DD2 spectrometer. The ^1H NMR (400 MHz) chemical shifts were measured relative to CDCl_3 as the internal reference (CDCl_3 : $\delta = 7.26$ ppm). The ^{13}C NMR (100 MHz) chemical shifts were given using CDCl_3 as the internal standard (CDCl_3 : $\delta = 77.16$ ppm). High-resolution mass spectra (HRMS) were obtained with a Shimadzu LCMS-IT-TOF (ESI). X-Ray single-crystal diffraction data were collected on an Oxford Xcalibur E (**6-PXZ-PRB**) and Bruker D8 VENTURE (**6-PXZ-PR**) single crystal diffraction. UV-Vis spectra were measured on a HITACHI U-2910. Fluorescence spectra, phosphorescence spectra and photoluminescence quantum yield were collected on a Horiba Jobin Yvon-Edison Fluoromax-3 fluorescence spectrometer with a calibrated integrating sphere system. Transient photoluminescence decay spectra were obtained with Horiba Single Photon Counting Controller: FluoroHub and Horiba TBX Picosecond Photon Detection. Thermogravimetric analysis (TGA) were carried out using DTG-60(H) at a rate of $10\text{ }^\circ\text{C}/\text{min}$ under nitrogen atmosphere. Differential scanning calorimetry (DSC) thermograms were recorded on DSC 200PC equipment under nitrogen atmosphere at a rate of $10\text{ }^\circ\text{C}/\text{min}$. Cyclic voltammogram were performed on LK2005A

with a solution of tetrabutylammonium hexafluorophosphate (Bu_4NPF_6 , 0.1 M) in DMF as electrolyte and ferrocene/ferrocenium (Fc/Fc^+) as standard. Three-electrode system (Ag/Ag^+ , platinum wire and glassy carbon electrode as reference, counter and work electrode respectively) was used in the CV measurement.

II. OLED Fabrication and Characterization

ITO (indium tin oxide) glass substrates with a sheet resistance of 15Ω per square were cleaned with alkaline detergent, boiled deionized water, and deionized water thoroughly in ultrasonic bath and then treated with O_2 plasma for 10 min. All the organic layers were deposited onto the ITO-coated substrates by thermal evaporation in a high vacuum chamber below 5×10^{-4} mbar in an inert gas glovebox. The quartz crystal oscillators controlled the thicknesses of deposited films. The as-fabricated OLEDs were measured in the inert gas glovebox without any encapsulation. Current density of OLEDs was measured by KEYSIGHT B1500A. The luminance and EL spectra were collected with model DLM-100Z photometer and OPT2000 spectrophotometer, respectively.

III. Theoretical Calculation

All theoretical calculations were performed using Gaussian 09 serials software. The ground-state structures and FMOs were obtained by B3LYP^{1,2} density functional method with basis set 6-31G*. The S_1 and T_1 energies were calculated by time-dependent DFT (TD-DFT) method with the same parameters for ground-state calculations. The HOMO and LUMO distributions were visualized using Gaussview 5.0 software. Natural Transition Orbital (NTO) analysis were carried out on S_1

and T₁ geometry under CAM-B3LYP/6-31G(d) method³. In addition, the polarizable continuum model (PCM) was applied to take account of the polarization effect of the solid-state environment with taking the toluene as reference solvent. Electron densities were calculated by using Multiwfn 3.7 program with crystal geometry⁴.

IV. Synthesis and Characterization

2-chloro-6,9-diphenyl-9H-purine (3): A dried round bottle flask with a magnetic stir bar was charged with 2,6-dichloro-9-phenyl-9H-purine (3.18 g, 12 mmol), Pd(PPh₃)₄ (693.3 mg, 0.6 mmol), phenylboronic acid (1.46 g, 12 mmol), K₂CO₃ (4.98 g, 36 mmol) and toluene 100 mL under a N₂ atmosphere. The resulting mixture was stirred at 80 °C for 24 h. Then the solution was filtered through a celite pad and washed with dichloromethane. The filtrate was evaporated under reduced pressure and the residue was purified by column chromatography on silica gel (petroleum ether/ethyl acetate = 10:1, v/v) to provide compound **3** as a white solid in 55 % yield (2.02 g, 6.6 mmol). ¹H NMR (400 MHz, CDCl₃) δ (ppm): 8.86-8.78 (m, 2H), 8.37 (s, 1H), 7.75-7.70 (m, 2H), 7.65-7.56 (m, 5H), 7.51 (t, *J* = 7.4 Hz, 1H); ¹³C NMR (100 MHz, CDCl₃) δ (ppm): 157.4, 155.0, 153.8, 144.0, 134.5, 134.0, 132.0, 130.6, 130.23, 130.20, 128.92, 128.90, 123.8; HRMS (ESI) *m/z*: [M+H]⁺ calcd for C₁₇H₁₂ClN₄⁺, 307.0745; found, 307.0746.

2-chloro-6-(4-(10H-phenoxazin-10-yl)phenyl)-9-phenyl-9H-purine (4): Compound **4** was synthesized according to the same procedure as described above for the synthesis of **3**, except that [4-(10H-phenoxazin-10-yl)phenyl]boronic acid (3.64 g, 12 mmol) was used as the reactant instead

of phenylboronic acid. After the solvent was removed, the mixture was purified by column chromatography on silica gel (petroleum ether/dichloromethane = 1:1, v/v) to provide compound **4** as a yellow solid in 64% yield (3.75 g, 7.68 mmol). ¹H NMR (400 MHz, CDCl₃) δ (ppm): 9.03 (d, *J* = 7.9 Hz, 2H), 8.41 (s, 1H), 7.75 (d, *J* = 7.4 Hz, 2H), 7.59 (dd, *J* = 24.9, 17.1 Hz, 5H), 6.82-6.47 (m, 6H), 6.05 (d, *J* = 7.3 Hz, 2H); ¹³C NMR (100 MHz, CDCl₃) δ (ppm): 156.2, 155.2, 154.0, 144.4, 144.0, 142.3, 134.6, 134.0, 133.9, 132.9, 131.4, 130.7, 130.3, 129.1, 123.8, 123.4, 121.8, 115.7, 113.5; HRMS (ESI) *m/z*: [M+H]⁺ calcd for C₂₉H₁₉ClN₅O⁺, 488.1273; found, 488.1277.

2-(4-(10*H*-phenoxazin-10-yl)phenyl)-6,9-diphenyl-9*H*-purine (2-PXZ-PR): A dried round bottle flask with a magnetic stir bar was charged with 2-chloro-6,9-diphenyl-9*H*-purine (1.07 g, 3.5 mmol), Pd(PPh₃)₄ (202.2 mg, 0.175 mmol), [4-(10*H*-phenoxazin-10-yl)phenyl]boronic acid (2.12 g, 7 mmol), K₂CO₃ (1.45 g, 10.5 mmol) and toluene 35 mL under a N₂ atmosphere. The resulting mixture was refluxed at 150 °C for 24 h. Then the solution was filtered through a celite pad and washed with dichloromethane. The filtrate was evaporated under reduced pressure and the residue was purified by column chromatography on silica gel (petroleum ether/ethyl acetate = 10:1, v/v) to provide compound **2-PXZ-PR** as a yellow solid in 97 % yield (1.8 g, 3.4 mmol). ¹H NMR (400 MHz, CDCl₃) δ (ppm): 8.99 (d, *J* = 6.9 Hz, 2H), 8.86 (d, *J* = 8.3 Hz, 2H), 8.44 (s, 1H), 7.90 (d, *J* = 7.4 Hz, 2H), 7.70-7.57 (m, 5H), 7.51 (dd, *J* = 20.4, 7.9 Hz, 3H), 6.66 (dd, *J* = 42.1, 7.6 Hz, 6H), 6.04 (d, *J* = 7.6 Hz, 2H); ¹³C NMR (100 MHz, CDCl₃) δ (ppm): 158.5, 155.2, 153.3, 144.1, 143.6, 138.5, 135.6, 134.8, 131.34, 131.28, 130.5, 130.1, 130.0, 128.9, 128.5, 123.6, 123.4, 121.5, 115.6, 115.5, 113.5; HRMS (ESI) *m/z*: [M+H]⁺ calcd for C₃₅H₂₄N₅O⁺, 530.1975; found, 530.1974.

6-(4-(10H-phenoxazin-10-yl)phenyl)-2,9-diphenyl-9H-purine (6-PXZ-PR): A dried round bottle flask with a magnetic stir bar was charged with 2-chloro-6-(4-(10H-phenoxazin-10-yl)phenyl)-9-phenyl-9H-purine (1.95 g, 4 mmol), Pd(PPh₃)₄ (231.1 mg, 0.2 mmol), phenylboronic acid (975.4 mg, 8 mmol), K₂CO₃ (1.66 g, 12 mmol) and toluene 40 mL under a N₂ atmosphere. The resulting mixture was refluxed at 150 °C for 24 h. Then the solution was filtered through a celite pad and washed with dichloromethane. After the solvent was removed, the mixture was purified by column chromatography on silica gel (petroleum ether/ethyl acetate = 15:1, v/v) to provide compound **6-PXZ-PR** as a yellow solid in 87% yield (1.84 g, 3.48 mmol). ¹H NMR (400 MHz, CDCl₃) δ (ppm): 9.18 (d, *J* = 8.5 Hz, 2H), 8.68 (d, *J* = 6.4 Hz, 2H), 8.44 (s, 1H), 7.92 (d, *J* = 8.2 Hz, 2H), 7.67 (t, *J* = 8.0 Hz, 2H), 7.61 (d, *J* = 8.5 Hz, 2H), 7.57-7.47 (m, 4H), 6.75-6.59 (m, 6H), 6.14-6.06 (m, 2H); ¹³C NMR (100 MHz, CDCl₃) δ (ppm): 159.6, 154.0, 153.4, 144.1, 143.6, 141.5, 138.1, 136.3, 134.9, 134.2, 132.7, 131.2, 130.54, 130.46, 130.0, 128.7, 128.6, 128.4, 123.6, 123.4, 121.6, 115.7, 113.6; HRMS (ESI) *m/z*: [M+H]⁺ calcd for C₃₅H₂₄N₅O⁺, 530.1975; found, 530.1977.

2,6,9-triphenyl-9H-purine (5): A dried round bottle flask with a magnetic stir bar was charged with 2,6-dichloro-9-phenyl-9H-purine (3.18 g, 12 mmol), Pd(PPh₃)₄ (693.4 mg, 0.6 mmol), phenylboronic acid (4.39 g, 36 mmol), K₂CO₃ (4.97 g, 36 mmol) and toluene 50 mL under a N₂ atmosphere. The resulting mixture was refluxed at 150 °C for 24 h. Then the solution was filtered through a celite pad and washed with dichloromethane. The filtrate was evaporated under reduced pressure and the residue was purified by column chromatography on silica gel (petroleum

ether/ethyl acetate = 10:1, v/v) to provide compound **5** as a white solid in 67 % yield (2.78 g, 8 mmol). ¹H NMR (400 MHz, CDCl₃) δ (ppm): 9.01-8.92 (m, 2H), 8.66 (dd, *J* = 7.7, 1.3 Hz, 2H), 8.39 (s, 1H), 7.88 (d, *J* = 7.9 Hz, 2H), 7.68-7.56 (m, 5H), 7.51 (q, *J* = 8.6, 7.5 Hz, 4H); ¹³C NMR (100 MHz, CDCl₃) δ (ppm): 159.3, 155.0, 153.2, 143.2, 138.3, 136.2, 134.9, 131.1, 130.3, 130.0, 129.95, 128.8, 128.5, 128.2, 123.5; HRMS (ESI) *m/z*: [M+H]⁺ calcd for C₂₃H₁₇N₄⁺, 349.1448; found, 349.1448.

2-(4-(10*H*-phenoxazin-10-yl)phenyl)-6,8,9-triphenyl-9*H*-purine (2-PXZ-PRB): A dried round bottle flask with a magnetic stir bar was charged with **2-PXZ-PR** (1.06 g, 2 mmol), Pd(OAc)₂ (22.5 mg, 0.1mmol), CuI (1.14 g, 6 mmol), iodobenzene (0.45 mL, 4 mmol) and Cs₂CO₃ (1.63 g, 5 mmol) and DMF (20 mL) under a N₂ atmosphere. Reaction mixture was heated to 160 °C for 36 h. Then the solution was filtered through a celite pad and washed with dichloromethane. The solvent was evaporated under reduced pressure. Products were isolated by flash column chromatography (petroleum ether/ethyl acetate = 30:1, v/v) to provide compound **2-PXZ-PRB** as a yellow solid in 80% yield (968 mg, 1.6 mmol). ¹H NMR (400 MHz, CDCl₃) δ (ppm): 9.13 (d, *J* = 7.1 Hz, 2H), 8.80 (d, *J* = 8.1 Hz, 2H), 7.74-7.68 (m, 2H), 7.65 (t, *J* = 7.3 Hz, 2H), 7.61-7.51 (m, 4H), 7.51-7.35 (m, 7H), 6.65 (dd, *J* = 42.9, 7.6 Hz, 6H), 6.02 (d, *J* = 6.8 Hz, 2H); ¹³C NMR (100 MHz, CDCl₃) δ (ppm): 157.9, 156.1, 154.3, 153.9, 144.0, 140.4, 138.7, 136.3, 135.2, 134.4, 131.2, 131.1, 130.8, 130.6, 130.1, 129.9, 129.7, 129.4, 129.0, 128.8, 128.7, 127.8, 123.38, 121.43, 115.5, 113.5; HRMS (ESI) *m/z*: [M+H]⁺ calcd for C₄₁H₂₈N₅O⁺, 606.2288; found, 606.2289.

6-(4-(10H-phenoxazin-10-yl)phenyl)-2,8,9-triphenyl-9H-purine (6-PXZ-PRB): The same procedure as described above for the synthesis of **2-PXZ-PRB**, except that **6-PXZ-PR** (1.06 g, 2 mmol) was used as the reactant instead of **2-PXZ-PR**. After the solvent was removed, the mixture was purified by column chromatography on silica gel (petroleum ether/ethyl acetate = 30:1, v/v) to provide compound **6-PXZ-PRB** as a yellow solid in 65% yield (786.5 mg, 1.3 mmol). ¹H NMR (400 MHz, CDCl₃) δ (ppm): 9.31 (d, *J* = 8.5 Hz, 2H), 8.65-8.59 (m, 2H), 7.74-7.68 (m, 2H), 7.63-7.53 (m, 5H), 7.52-7.43 (m, 6H), 7.39 (t, *J* = 7.3 Hz, 2H), 6.76-6.59 (m, 6H), 6.11 (d, *J* = 9.4 Hz, 2H); ¹³C NMR (100 MHz, CDCl₃) δ (ppm): 159.0, 156.2, 154.4, 152.6, 144.1, 141.2, 138.3, 136.6, 135.2, 134.3, 132.8, 131.1, 130.6, 130.3, 130.0, 129.9, 129.7, 129.3, 129.0, 128.7, 128.6, 128.4, 127.8, 123.4, 121.6, 115.6, 113.6; HRMS (ESI) *m/z*: [M+H]⁺ calcd for C₄₁H₂₈N₅O⁺, 606.2288; found, 606.2289.

8-(4-(10H-phenoxazin-10-yl)phenyl)-2,6,9-triphenyl-9H-purine (8-PXZ-PRB): DMF (60 mL) was added to a dried round bottle flask with a magnetic stir bar, the flask containing a 2,6,9-triphenyl-9H-purine (2.09 g, 6 mmol), Pd(OAc)₂ (67.4 mg, 0.3 mmol), CuI (3.43 g, 18 mmol), 10-(4-bromophenyl)-10H-phenoxazine (4.06 g, 12 mmol.) and Cs₂CO₃ (4.90 g, 15 mmol) under a N₂ atmosphere. Reaction mixture was heated to 160 °C for 36 h. Then the solution was filtered through a celite pad and washed with dichloromethane. The solvent was evaporated under reduced pressure. Products were isolated by flash column chromatography (petroleum ether/ethyl acetate = 20:1, v/v) to provide compound **8-PXZ-PRB** as a yellow solid in 40% yield (1.43 g, 2.36 mmol). ¹H NMR (400 MHz, CDCl₃) δ (ppm): 9.13 (d, *J* = 8.1 Hz, 2H), 8.62 (d, *J* = 7.5 Hz, 2H),

7.92 (d, $J = 8.3$ Hz, 2H), 7.70-7.55 (m, 6H), 7.55-7.42 (m, 5H), 7.37 (d, $J = 8.4$ Hz, 2H), 6.77-6.51 (m, 6H), 5.96 (d, $J = 7.8$ Hz, 2H); ^{13}C NMR (100 MHz, CDCl_3) δ (ppm): 159.1, 156.1, 154.1, 152.8, 144.1, 141.0, 138.4, 136.4, 135.1, 133.9, 132.4, 131.2, 131.1, 130.2, 130.1, 129.9, 129.8, 129.6, 129.2, 128.8, 128.53, 128.50, 127.8, 123.4, 121.8, 115.8, 113.4; HRMS (ESI) m/z : $[\text{M}+\text{H}]^+$ calcd for $\text{C}_{41}\text{H}_{28}\text{N}_5\text{O}^+$, 606.2288; found, 606.2283.

V. Crystal Data

Table S1. Crystal data for **6-PXZ-PRB**.

Identification code	6-PXZ-PRB
Empirical formula	C ₄₁ H ₂₇ N ₅ O
Formula weight	605.67
Temperature/K	293.15
Crystal system	orthorhombic
Space group	Fdd2
a/Å	68.307(4)
b/Å	30.2720(14)
c/Å	5.8721(4)
α/°	90
β/°	90
γ/°	90
Volume/Å ³	12142.3(12)
Z	16
ρ _{calc} /cm ³	1.325
μ/mm ⁻¹	0.082
F(000)	5056.0
Crystal size/mm ³	0.35 × 0.3 × 0.25
Radiation	MoKα (λ = 0.71073)
2θ range for data collection/°	5.888 to 52.738
Index ranges	-84 ≤ h ≤ 52, -23 ≤ k ≤ 37, -7 ≤ l ≤ 4
Reflections collected	8518
Independent reflections	4583 [R _{int} = 0.0252, R _{sigma} = 0.0448]
Data/restraints/parameters	4583/1/424
Goodness-of-fit on F ²	0.971
Final R indexes [I ≥ 2σ (I)]	R ₁ = 0.0394, wR ₂ = 0.0774
Final R indexes [all data]	R ₁ = 0.0597, wR ₂ = 0.0839
Largest diff. peak/hole / e Å ⁻³	0.14/-0.18
Flack parameter	-0.5(10)

Table S2. Crystal data for **6-PXZ-PR**.

Identification code	6-PXZ-PR
Empirical formula	C ₃₅ H ₂₃ N ₅ O
Formula weight	529.58
Temperature/K	296.0
Crystal system	triclinic
Space group	P-1
a/Å	9.2775(4)
b/Å	11.1468(6)
c/Å	26.0342(13)
α/°	85.694(2)
β/°	84.951(2)
γ/°	80.772(2)
Volume/Å ³	2642.1(2)
Z	4
ρ _{calc} /cm ³	1.331
μ/mm ⁻¹	0.083
F(000)	1104.0
Crystal size/mm ³	0.35 × 0.25 × 0.2
Radiation	MoKα (λ = 0.71073)
2θ range for data collection/°	3.938 to 55.108
Index ranges	-12 ≤ h ≤ 12, -14 ≤ k ≤ 14, -33 ≤ l ≤ 33
Reflections collected	68373
Independent reflections	12166 [R _{int} = 0.0824, R _{sigma} = 0.0535]
Data/restraints/parameters	12166/0/739
Goodness-of-fit on F ²	1.010
Final R indexes [I ≥ 2σ (I)]	R ₁ = 0.0531, wR ₂ = 0.1173
Final R indexes [all data]	R ₁ = 0.1161, wR ₂ = 0.1474
Largest diff. peak/hole / e Å ⁻³	0.14/-0.21

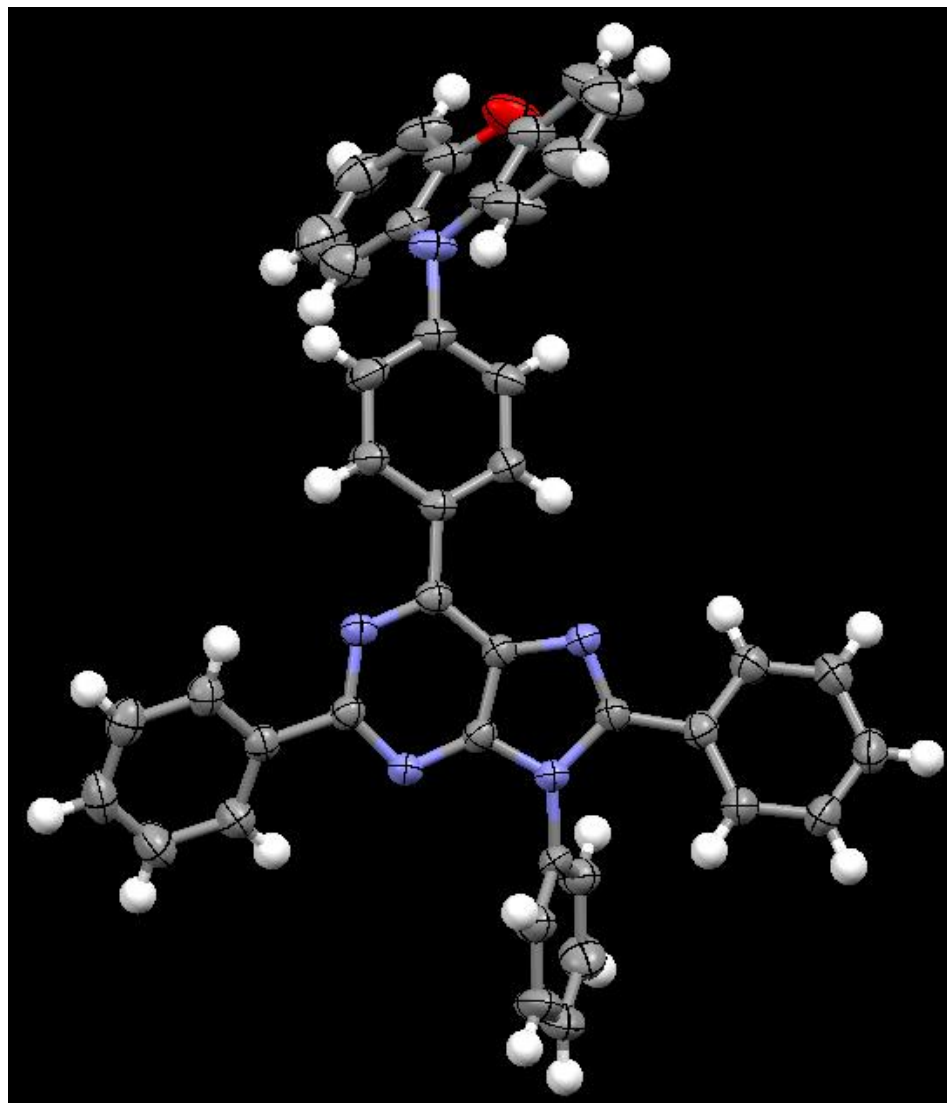


Figure S1. ORTEP diagram of the molecular structure of **6-PXZ-PRB** (CCDC: 2069566).

Thermal ellipsoids are shown at the 50% probability level.

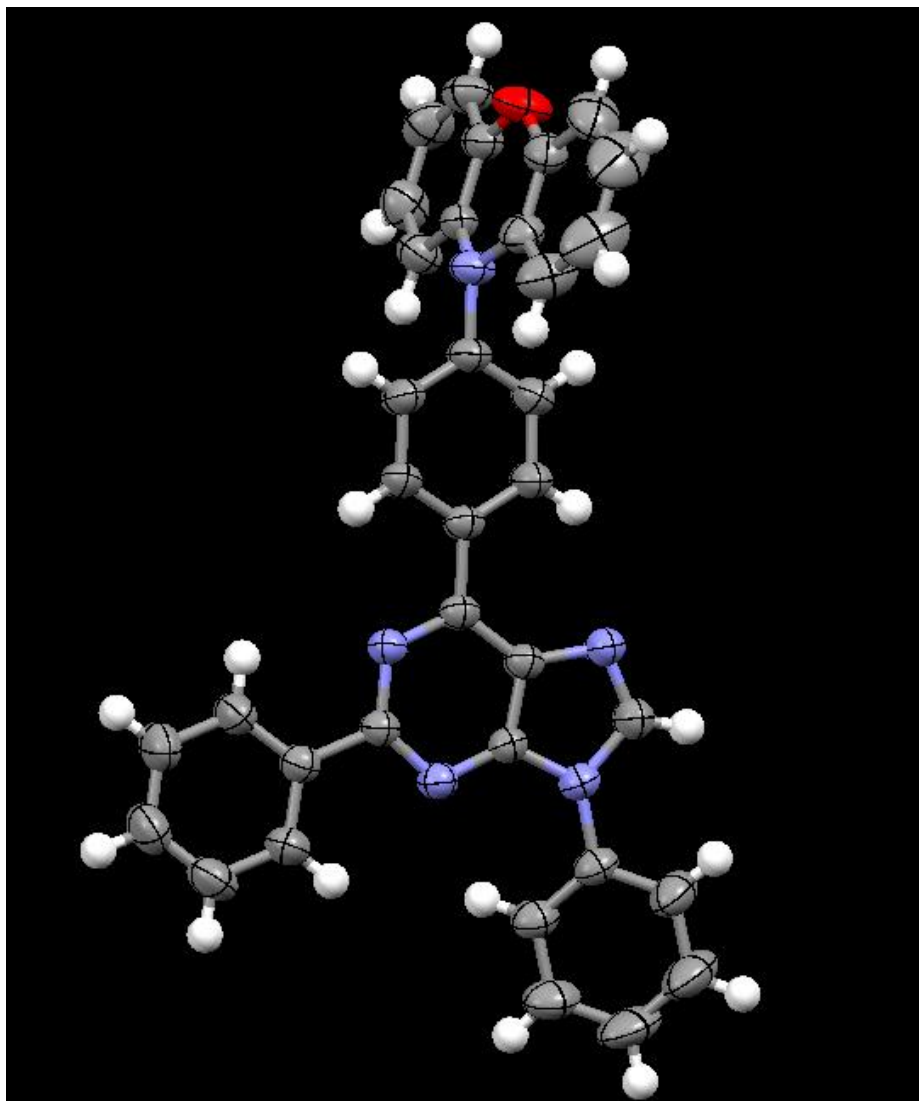


Figure S2. ORTEP diagram of the molecular structure of **6-PXZ-PR** (CCDC: 2069564). Thermal ellipsoids are shown at the 50% probability level.

VI. Additional Spectra and Data

Table S3. Theoretical calculation results of the FMOs distributions and energy levels of **2-PXZ-PRB**, **6-PXZ-PRB**, **8-PXZ-PRB**, **2-PXZ-PR** and **6-PXZ-PR**.

	HOMO (eV)	LUMO (eV)	E_g (eV)	S_1 (eV)	T_1 (eV)	ΔE_{ST} (eV)
2-PXZ-PRB	-4.34	-1.96	2.38	2.1876	2.1844	0.0032
6-PXZ-PRB	-4.52	-2.00	2.52	2.0826	2.0748	0.0078
8-PXZ-PRB	-4.73	-1.98	2.75	2.2909	2.2843	0.0066
2-PXZ-PR	-4.55	-1.89	2.67	2.2565	2.2517	0.0048
6-PXZ-PR	-4.55	-1.94	2.61	2.1182	2.1112	0.0070

Table S4. Summary of physical properties of **2-PXZ-PRB**, **6-PXZ-PRB**, **8-PXZ-PRB**, **2-PXZ-PR** and **6-PXZ-PR**.

	HOMO ^a (eV)	LUMO ^b (eV)	E_g^c (eV)
2-PXZ-PRB	-5.04	-2.28	2.76
6-PXZ-PRB	-5.06	-2.44	2.62
8-PXZ-PRB	-5.07	-2.40	2.67
2-PXZ-PR	-5.05	-2.30	2.75
6-PXZ-PR	-5.06	-2.45	2.61

^aMeasured in dry N,N-dimethylformamide solution, where $E_{HOMO} = -4.8 - (E_{ox} - E_{Fc})$. ^bEstimated according to the absorption spectra and the HOMO energy levels. ^cCalculated from the absorption spectra.

Table S5. Natural Transition Orbital (NTO) Analysis of S_1 and T_1 States.

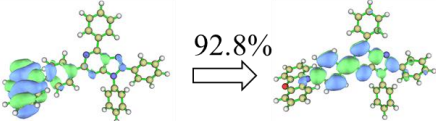
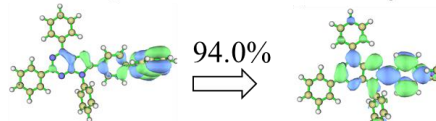
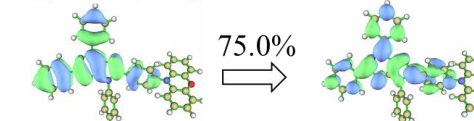
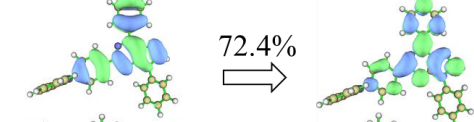
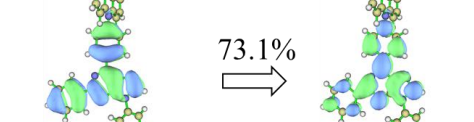
Compound	$S_0 \rightarrow S_1$		$S_0 \rightarrow T_1$	
2-PXZ-PRB		92.8%		75.2%
6-PXZ-PRB		91.2%		74.2%
8-PXZ-PRB		94.0%		75.0%
2-PXZ-PR		92.6%		72.4%
6-PXZ-PR		94.7%		73.1%

Table S6. Summary of fluorescent emission wavelength of **2-PXZ-PRB**-, **6-PXZ-PRB**-, **8-PXZ-PRB**-, **2-PXZ-PR**- and **6-PXZ-PR**-doped mCBP films (1-50 wt%) and neat films measured at room temperature.

Compound	1%	5%	10%	20%	30%	40%	50%	neat film
2-PXZ-PRB	484	486	496	504	504	508	506	510
6-PXZ-PRB	512	516	520	522	530	528	536	556
8-PXZ-PRB	492	498	508	512	514	518	518	522
2-PXZ-PR	474	492	488	496	495	500	504	502
6-PXZ-PR	506	514	514	522	522	524	530	528

Table S7. Photophysical characteristics of **2-PXZ-PRB**, **6-PXZ-PRB**, **8-PXZ-PRB**, **2-PXZ-PR** and **6-PXZ-PR**.

Compound	τ_p^a (ns)	τ_d^b (μ s)	$\Phi_{N_2}^c$ (%)	$\Phi_{O_2}^d$ (%)	C_1^e	C_2^f	k_{risc}^g ($\times 10^4$ s^{-1})	k_r^h ($\times 10^7$ s^{-1})	k_{isc}^i ($\times 10^7$ s^{-1})
2-PXZ-PRB	12.5	58.5	71	31	0.44	0.56	3.92	2.48	4.51
6-PXZ-PRB	14.8	48.1	54	29	0.54	0.46	3.87	1.96	3.13
8-PXZ-PRB	13.6	43.4	51	36	0.71	0.29	3.26	2.65	2.16
2-PXZ-PR	11.9	32.5	42	25	0.60	0.40	5.17	2.10	3.40
6-PXZ-PR	16.9	24.3	66	31	0.47	0.53	8.76	1.83	3.14

^aPrompt lifetime. ^bDelayed lifetime. ^cMeasured in toluene solution under N₂ atmosphere. ^dMeasured in toluene solution under O₂ atmosphere. ^eThe proportion of prompt components, calculated from $C_1 = \Phi_{O_2}/\Phi_{N_2}$. ^fThe proportion of delayed components, calculated from $C_2 = 1 - C_1$. ^gReverse intersystem crossing rate, calculated from $k_{risc} = 1/(C_1\tau_d)$. ^hRadiative decay rate of singlet, calculated from $k_r = C_1\Phi_{N_2}/\tau_p$. ⁱIntersystem crossing rate, calculated from $k_{isc} = (1 - C_1)/\tau_p$.

Table S8. Commission Internationale de l'Eclairage Coordinates of **2-PXZ-PRB**-, **6-PXZ-PRB**-, **8-PXZ-PRB**-, **2-PXZ-PR**- and **6-PXZ-PR**-based OLEDs measured at 5000 cd m⁻².

	2-PXZ-PRB	6-PXZ-PRB	8-PXZ-PRB	2-PXZ-PR	6-PXZ-PR
(x, y)	(0.31, 0.51)	(0.41, 0.54)	(0.35, 0.54)	(0.27, 0.49)	(0.37, 0.55)

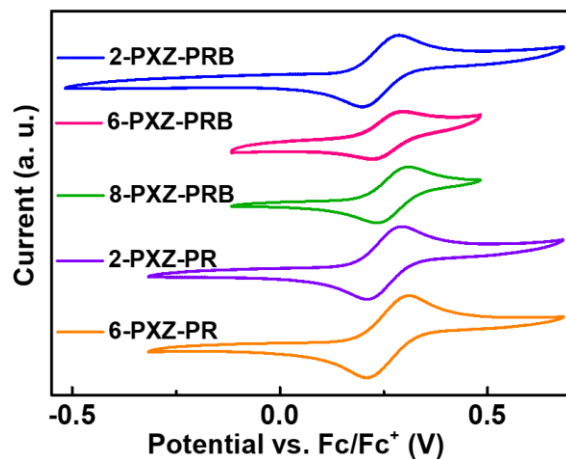


Figure S3. Cyclic voltammograms (CV) of **2-PXZ-PRB**, **6-PXZ-PRB**, **8-PXZ-PRB**, **2-PXZ-PR** and **6-PXZ-PR** measured in dry N,N-dimethylformamide solution containing 0.1 M of tetrabutylammonium hexafluorophosphate.

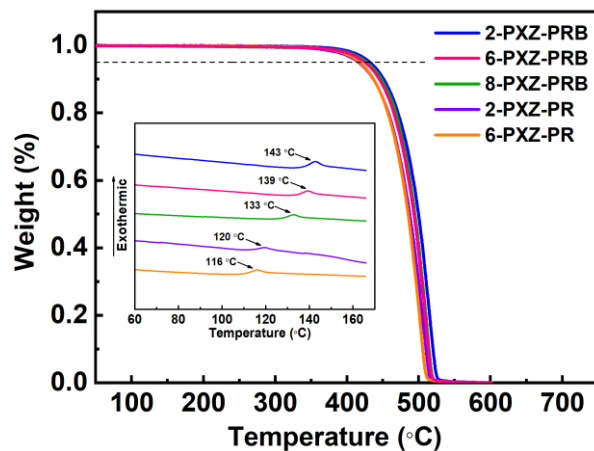


Figure S4. Thermogravimetry analysis (TGA) of **2-PXZ-PRB**, **6-PXZ-PRB**, **8-PXZ-PRB**, **2-PXZ-PR** and **6-PXZ-PR** recorded at a heating rate of 10 °C min⁻¹. Inset: Differential scanning calorimetry (DSC) of **2-PXZ-PRB**, **6-PXZ-PRB**, **8-PXZ-PRB**, **2-PXZ-PR** and **6-PXZ-PR** recorded at a heating rate of 10 °C min⁻¹.

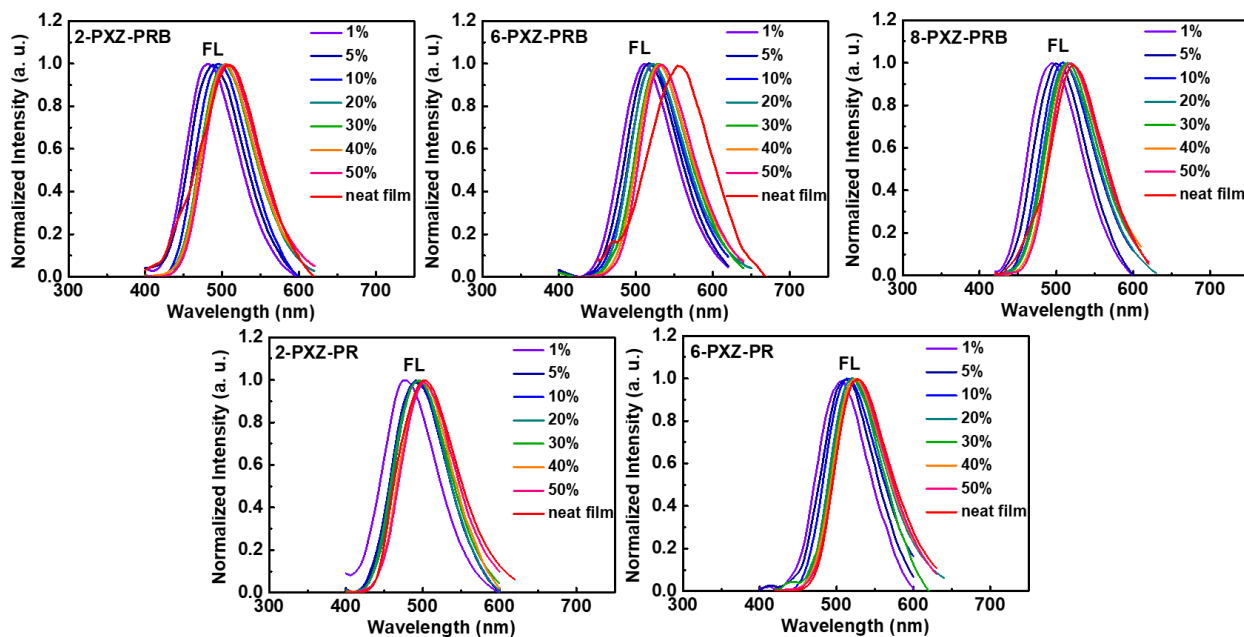


Figure S5. Fluorescence (FL) spectra of **2-PXZ-PRB-**, **6-PXZ-PRB-**, **8-PXZ-PRB-**, **2-PXZ-PR-** and **6-PXZ-PR-**doped mCBP films (1-50 wt%) and neat films measured at room temperature.

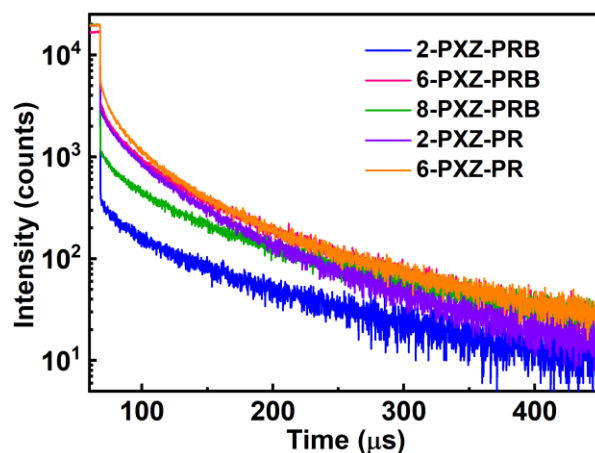


Figure S6. Transient photoluminescence curves of **2-PXZ-PRB-**, **6-PXZ-PRB-**, **8-PXZ-PRB-**, **2-PXZ-PR-** and **6-PXZ-PR-**doped mCBP films (20 wt%) measured at room temperature.

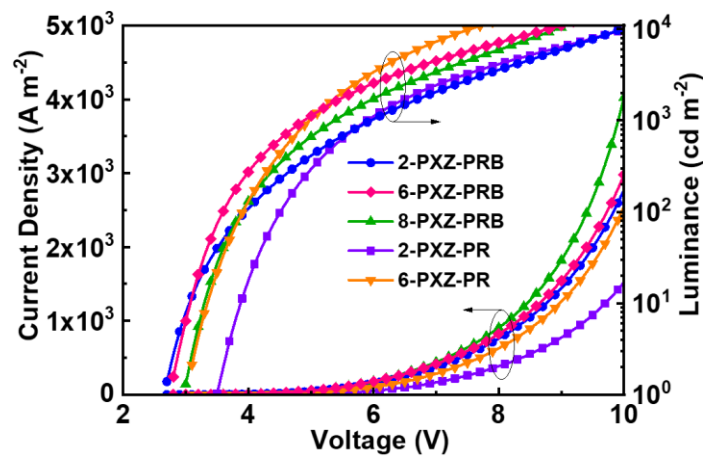


Figure S7. Current density-luminance-voltage characteristics of **2-PXZ-PRB**-, **6-PXZ-PRB**-, **8-PXZ-PRB**-, **2-PXZ-PR**- and **6-PXZ-PR**-based OLEDs.

VII. References

- (1) A. D. Becke, Density-functional thermochemistry. III. The role of exact exchange. *J. Chem. Phys.* **1993**, *98*, 5648-5652.
- (2) C. Lee, W. Yang, R. G. Parr, Development of the Colle-Salvetti correlation-energy formula into a functional of the electron density. *Phys. Rev. B.* **1988**, *37*, 785-789.
- (3) Samanta, P. K.; Kim, D.; Coropceanu, V.; Brédas, J.-L., Up-Conversion Intersystem Crossing Rates in Organic Emitters for Thermally Activated Delayed Fluorescence: Impact of the Nature of Singlet vs Triplet Excited States. *J. Am. Chem. Soc.* **2017**, *139*, 4042-4051.
- (4) Lu, T.; Chen, F., Multiwfn: A Multifunctional Wavefunction Analyzer. *J. Comput. Chem.* **2012**, *33*, 580-592.

VIII. Copies of NMR Spectra

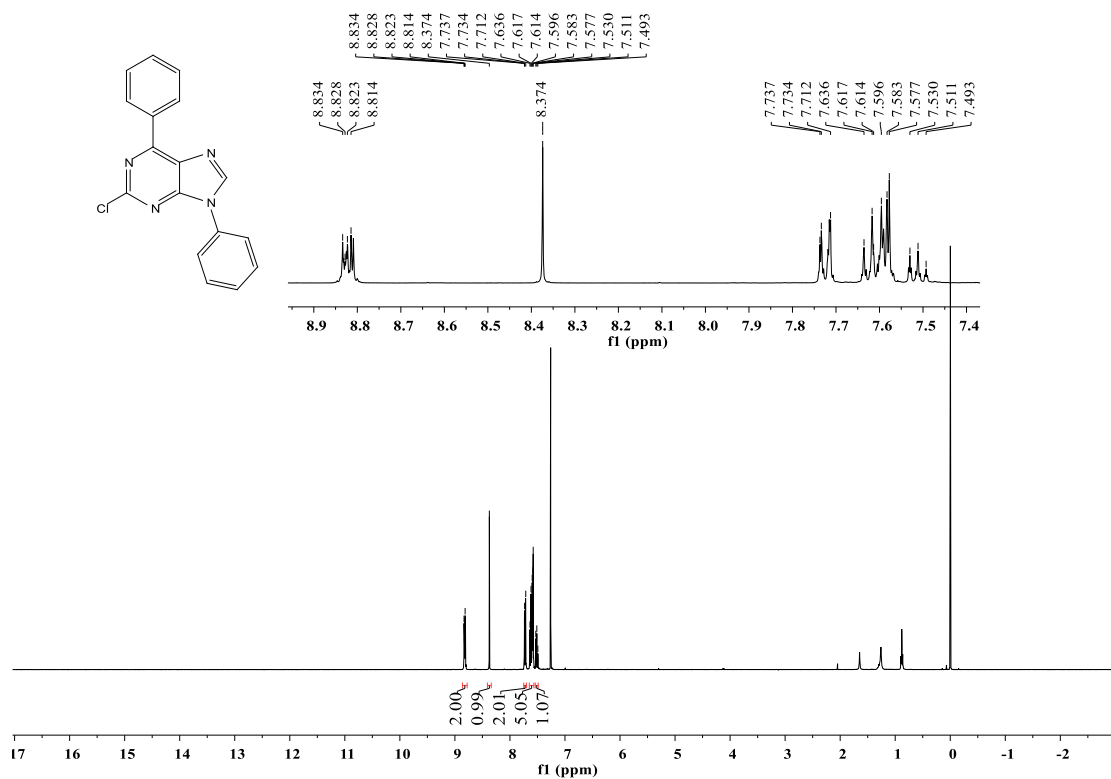


Figure S8. ¹H NMR (400 MHz) spectra of **3** in CDCl₃.

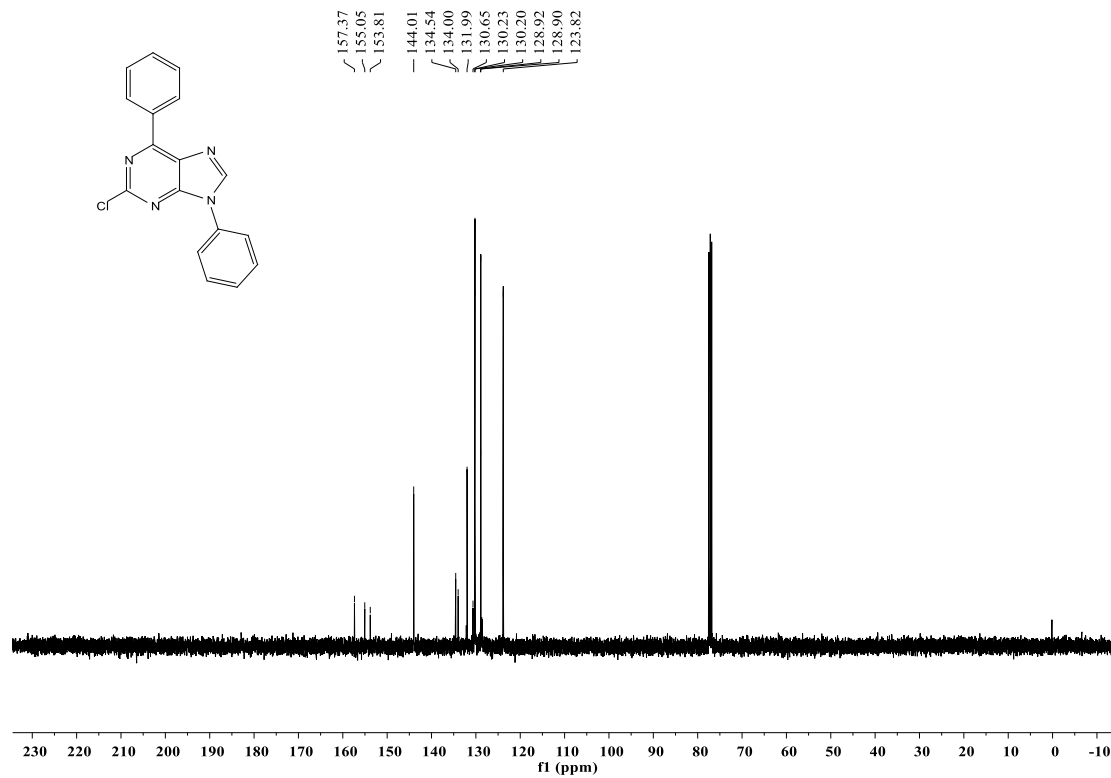


Figure S9. ¹³C NMR (100 MHz) spectra of **3** in CDCl₃.

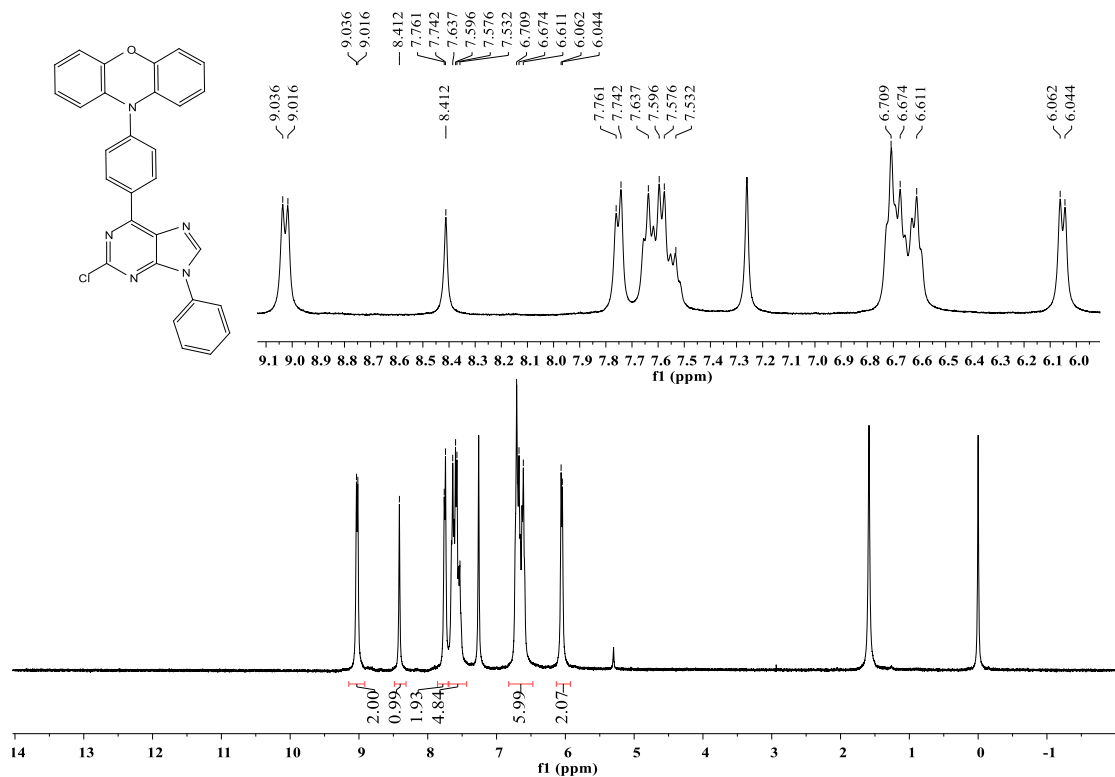


Figure S10. ¹H NMR (400 MHz) spectra of **4** in CDCl₃.

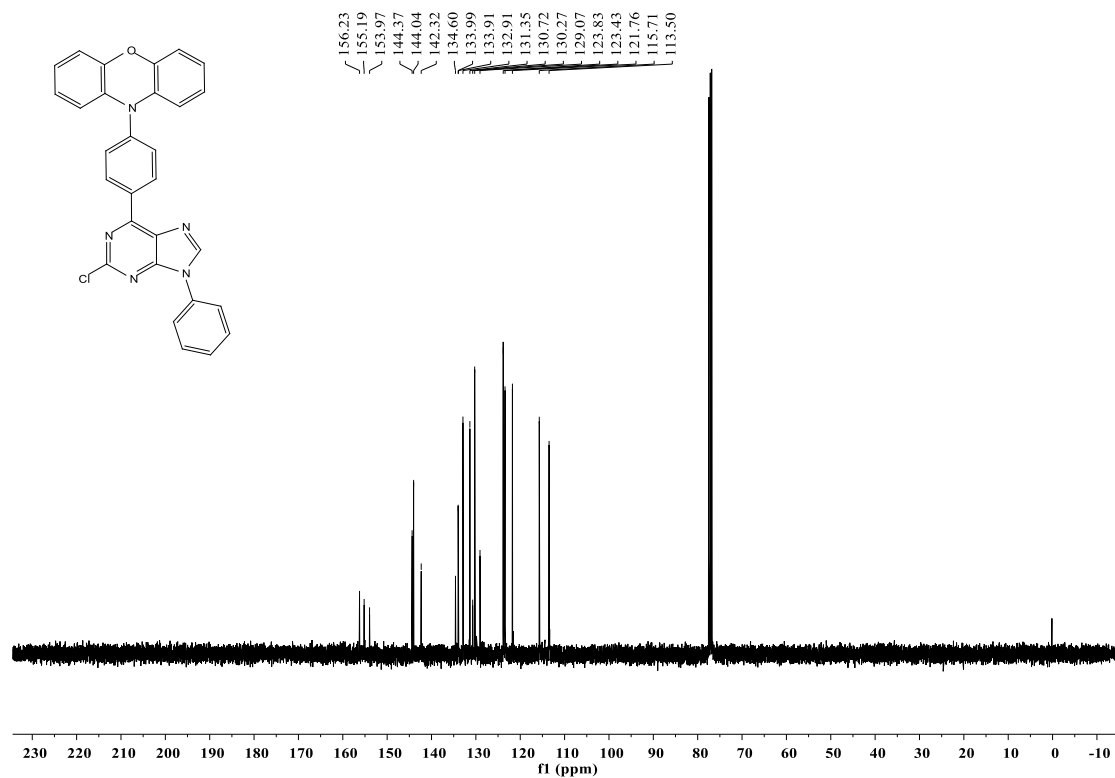


Figure S11. ¹³C NMR (100 MHz) spectra of **4** in CDCl₃.

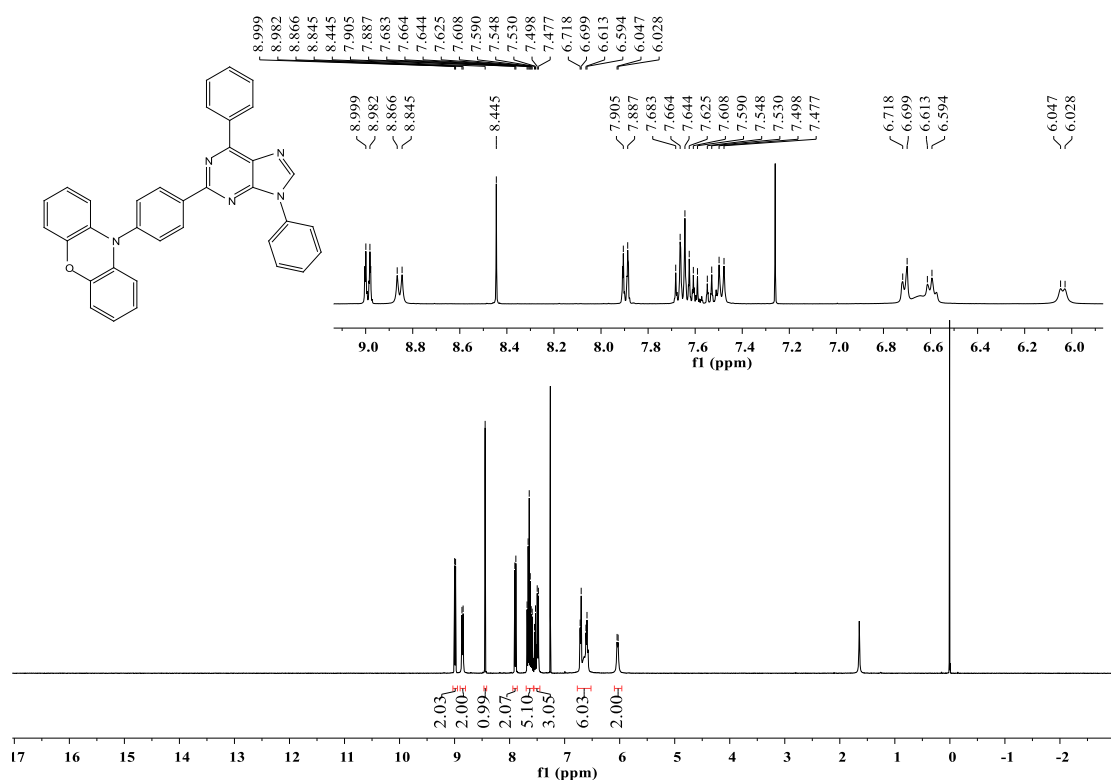


Figure S12. ¹H NMR (400 MHz) spectra of **2-PXZ-PR** in CDCl₃.

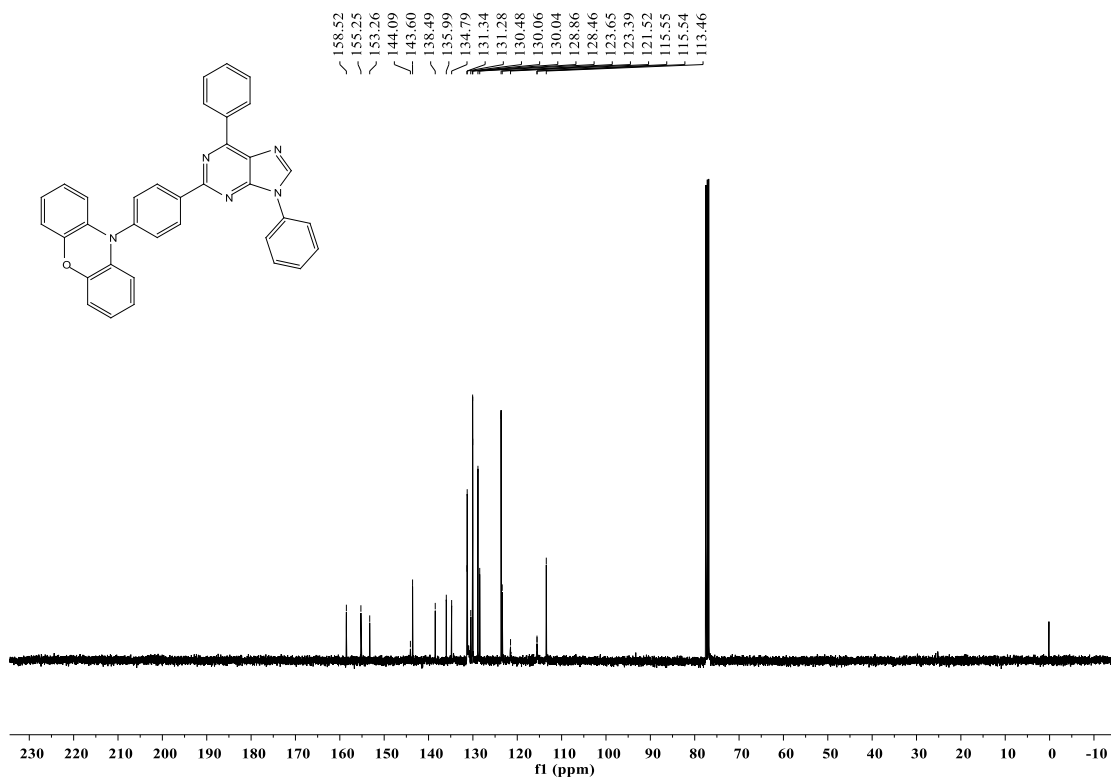


Figure S13. ¹³C NMR (100 MHz) spectra of **2-PXZ-PR** in CDCl₃.

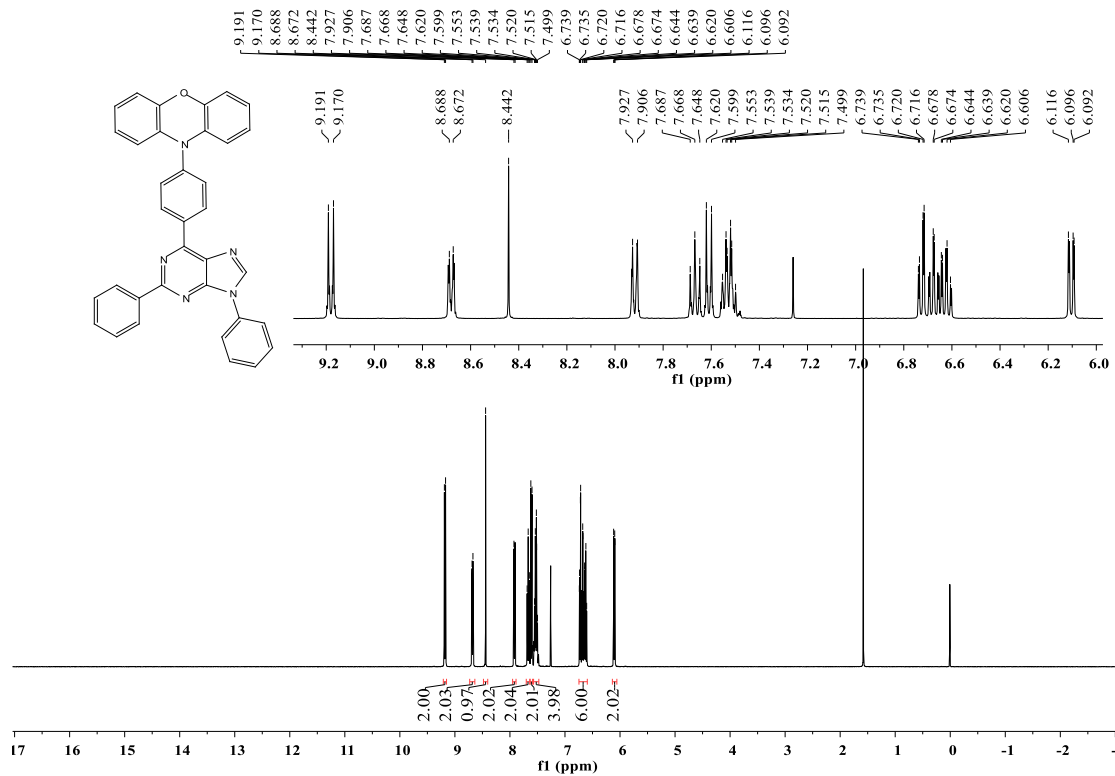


Figure S14. ¹H NMR (400 MHz) spectra of **6-PXZ-PR** in CDCl₃.

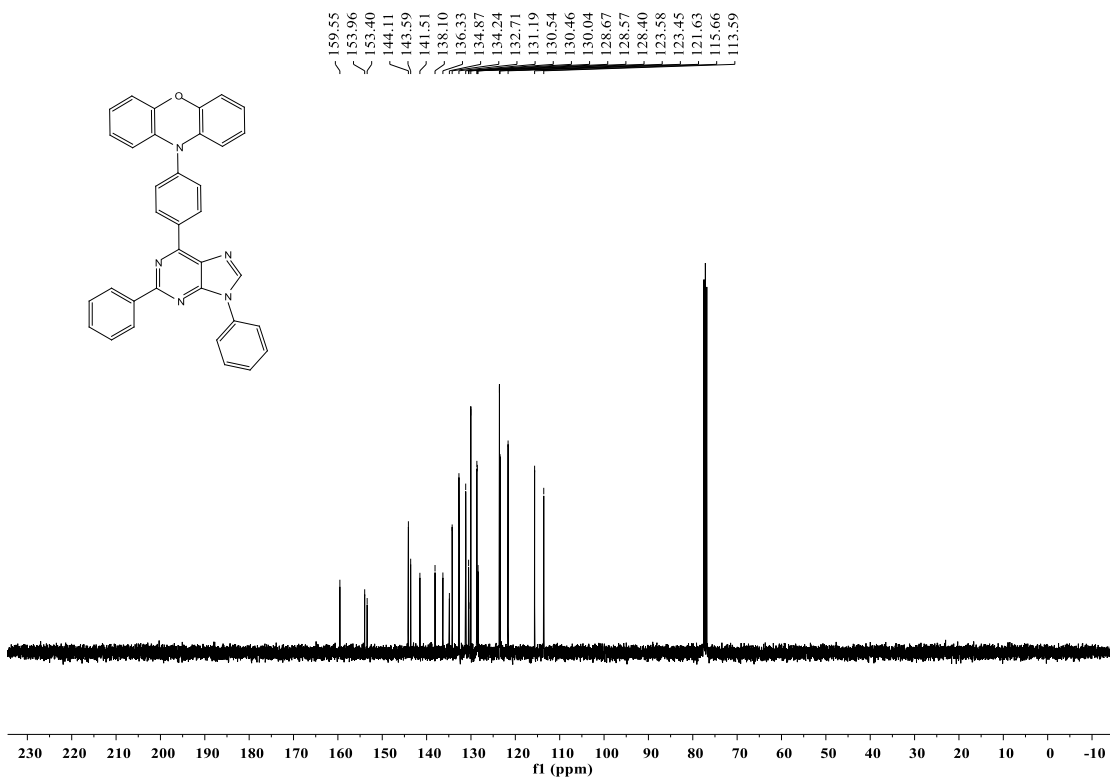


Figure S15. ¹³C NMR (100 MHz) spectra of **6-PXZ-PR** in CDCl₃.

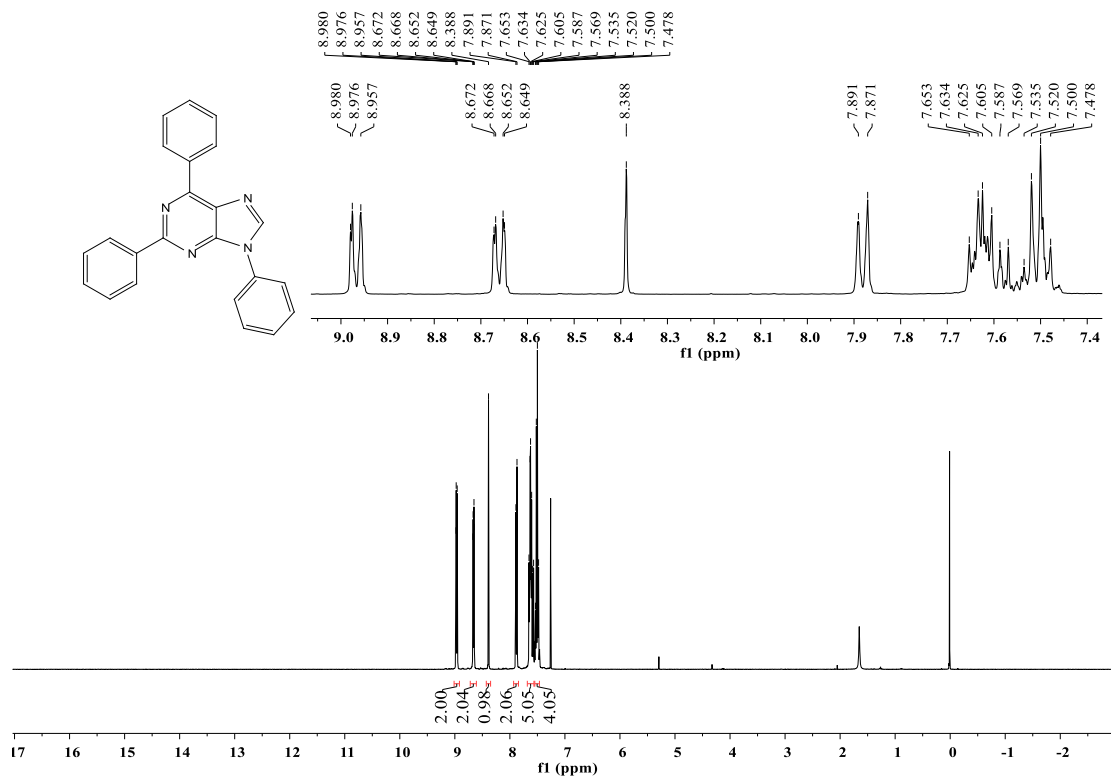


Figure S16. ¹H NMR (400 MHz) spectra of **5** in CDCl₃.

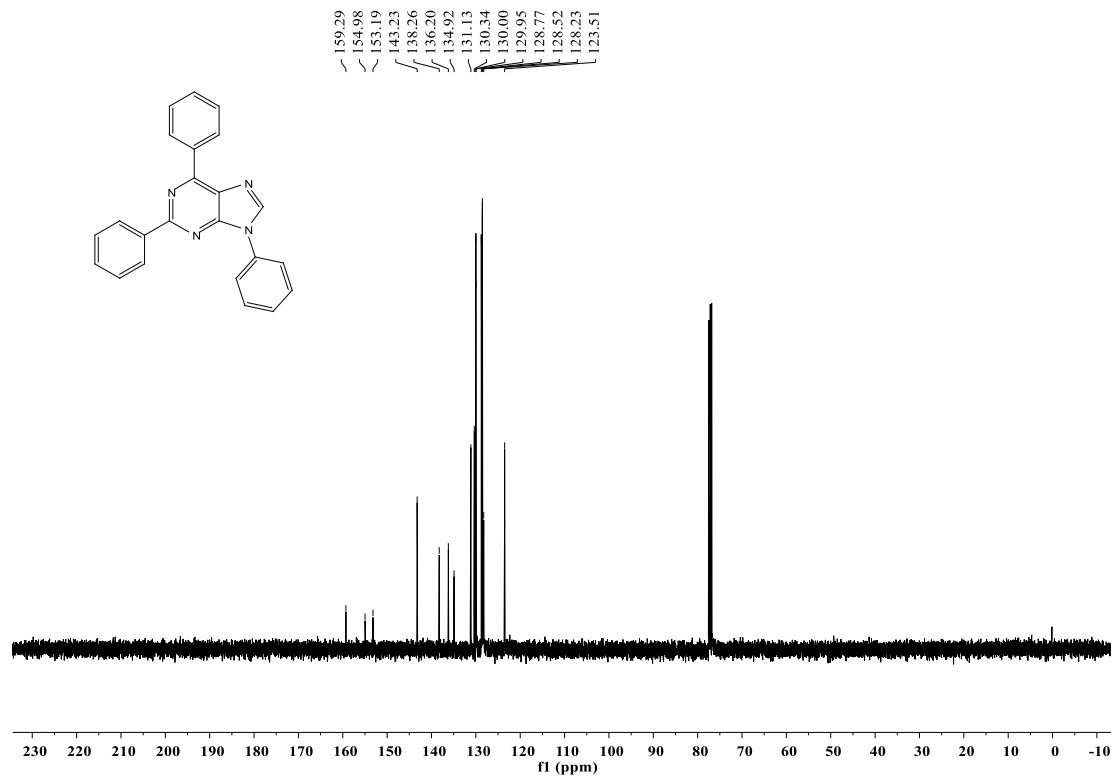


Figure S17. ¹³C NMR (100 MHz) spectra of **5** in CDCl₃.

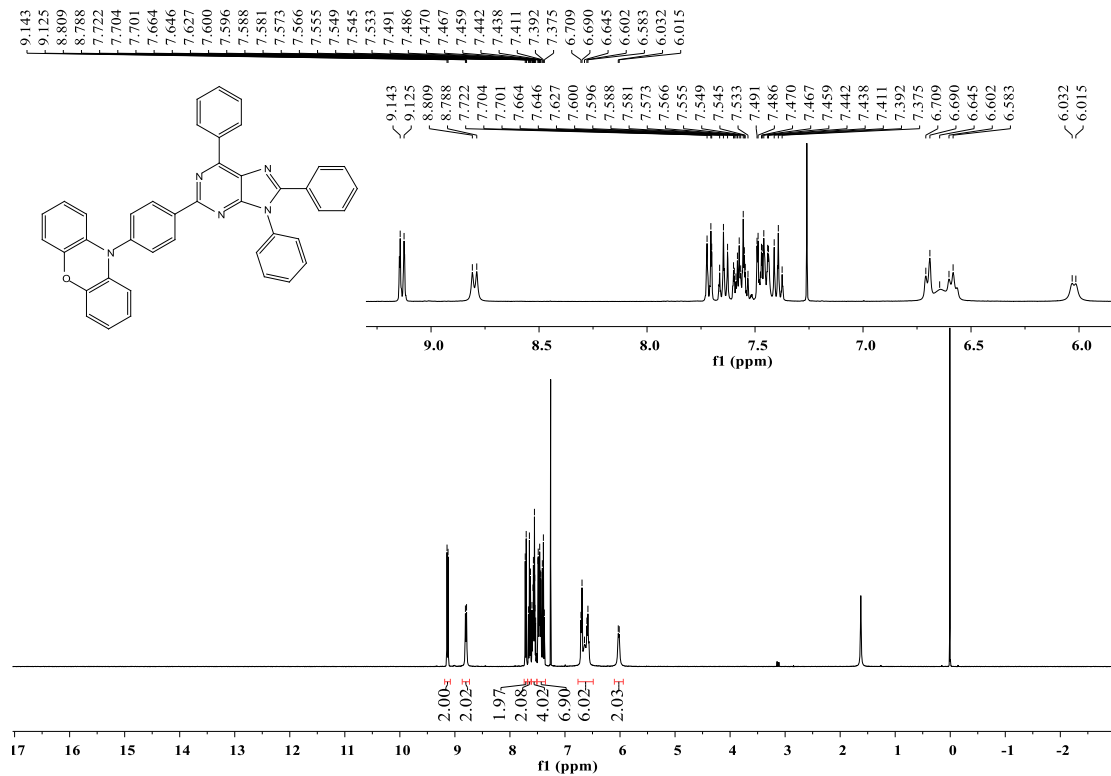


Figure S18. ¹H NMR (400 MHz) spectra of **2-PXZ-PRB** in CDCl₃.

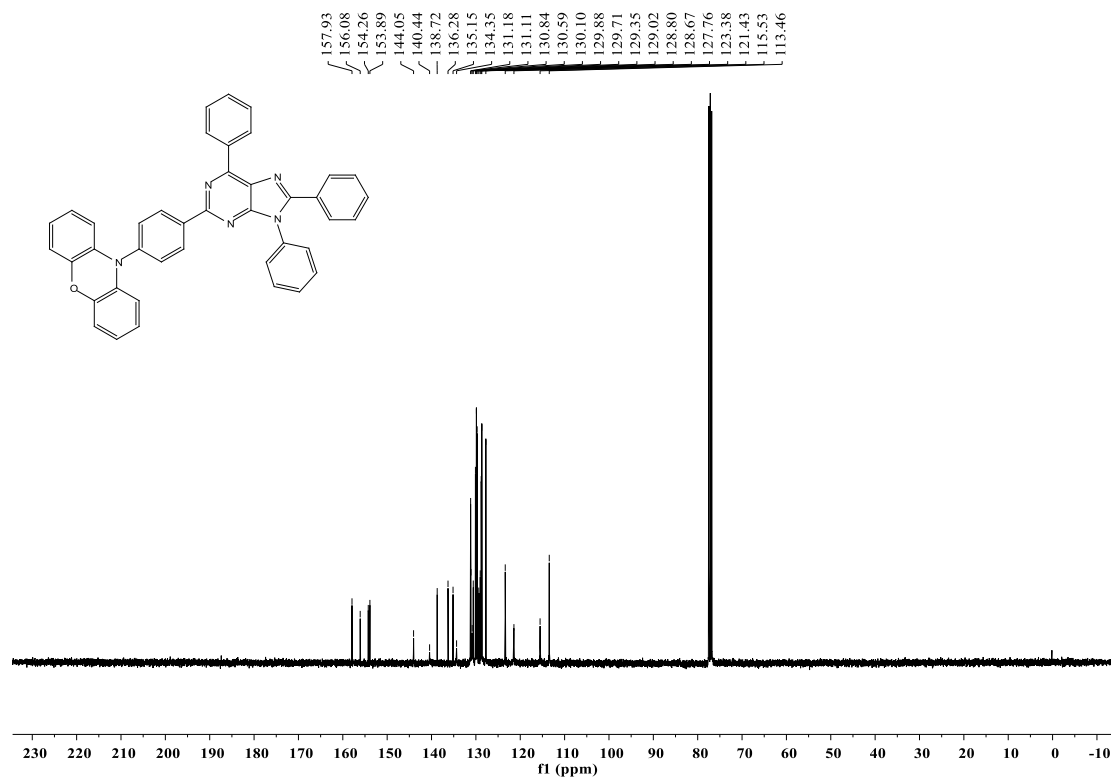


Figure S19. ¹³C NMR (100 MHz) spectra of **2-PXZ-PRB** in CDCl₃.

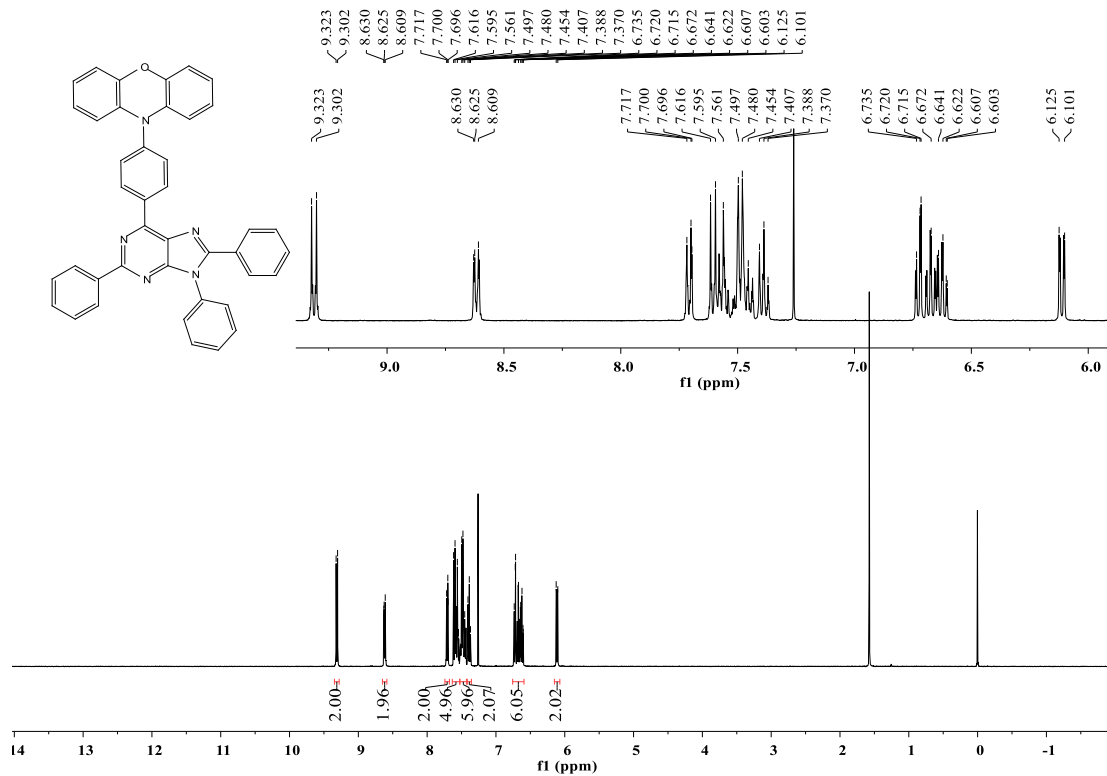


Figure S20. ¹H NMR (400 MHz) spectra of **6-PXZ-PRB** in CDCl₃.

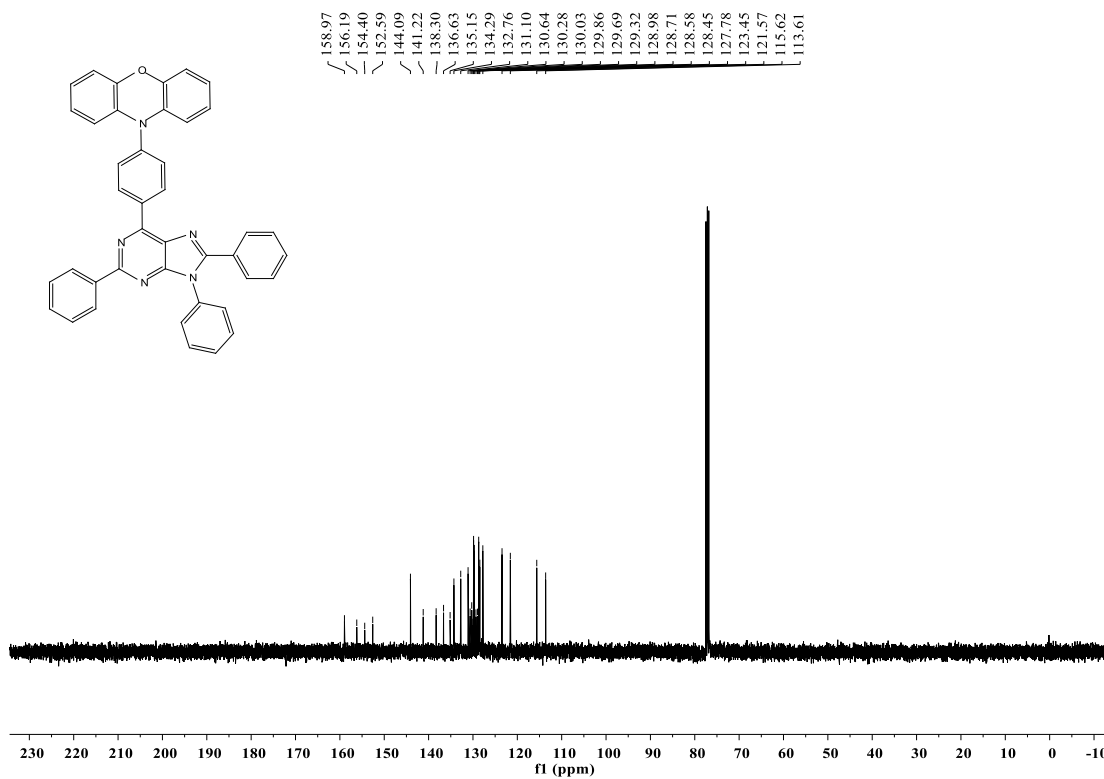


Figure S21. ¹³C NMR (100 MHz) spectra of **6-PXZ-PRB** in CDCl₃.

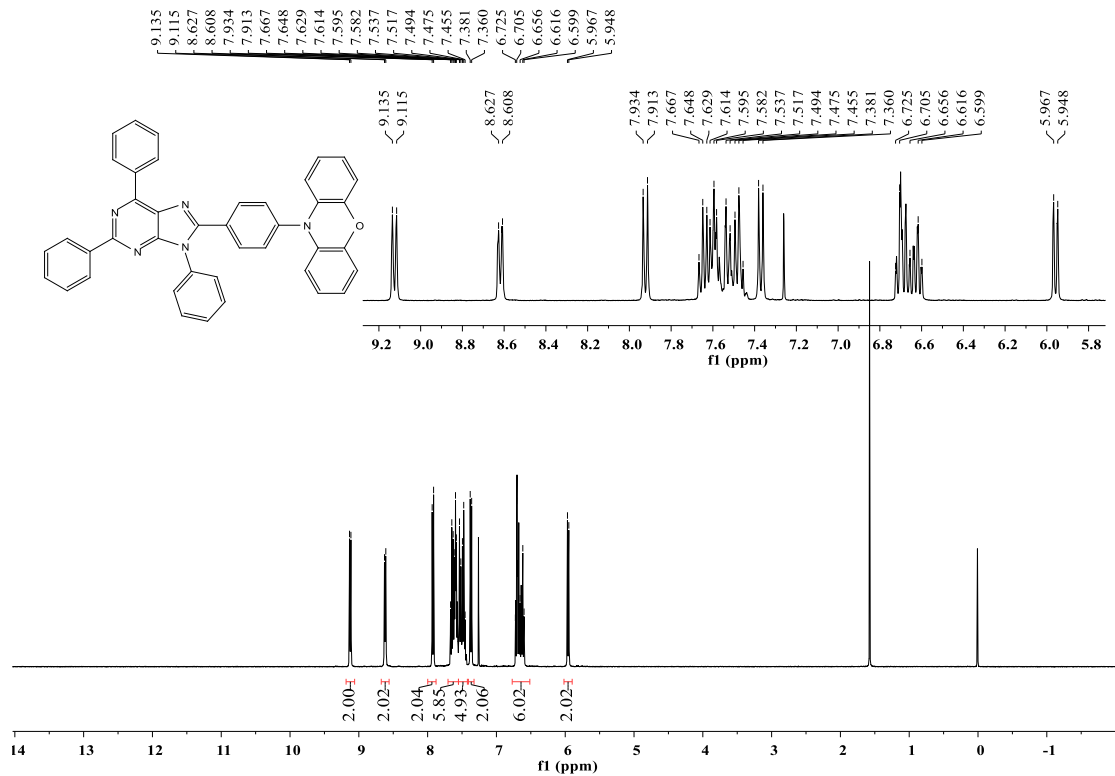


Figure S22. ¹H NMR (400 MHz) spectra of **8-PXZ-PRB** in CDCl₃.

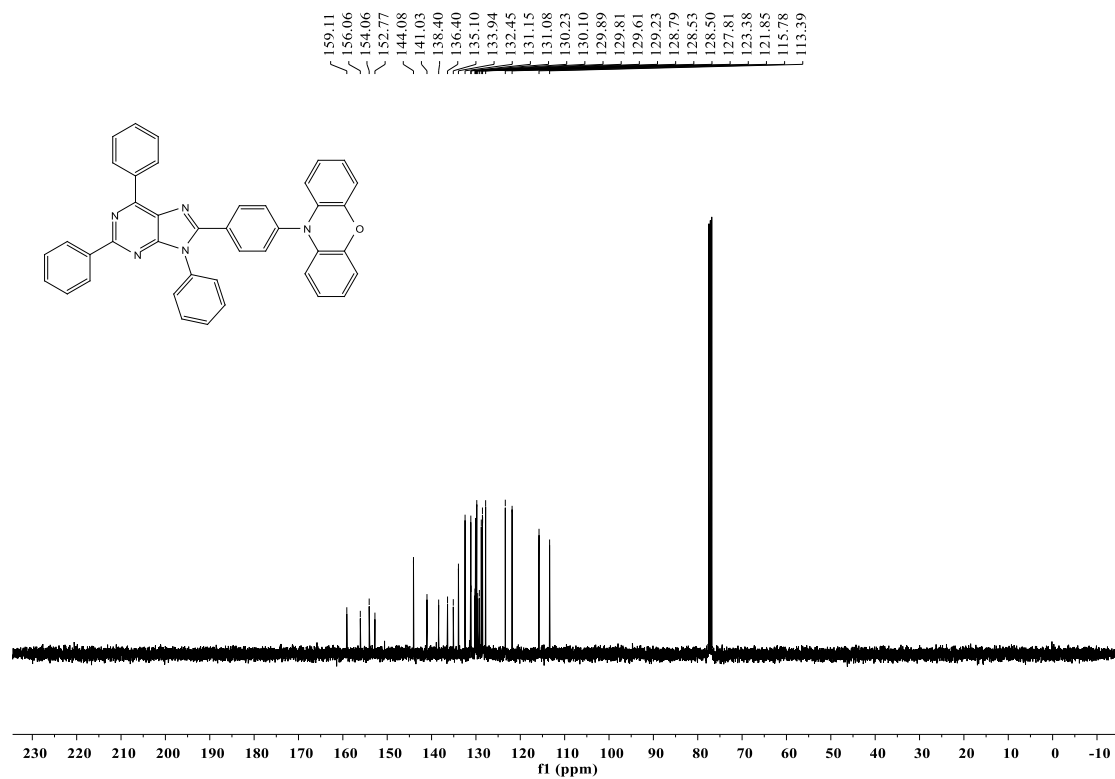


Figure S23. ¹³C NMR (100 MHz) spectra of **8-PXZ-PRB** in CDCl₃.

IX. Copies of High-Resolution Mass Spectra

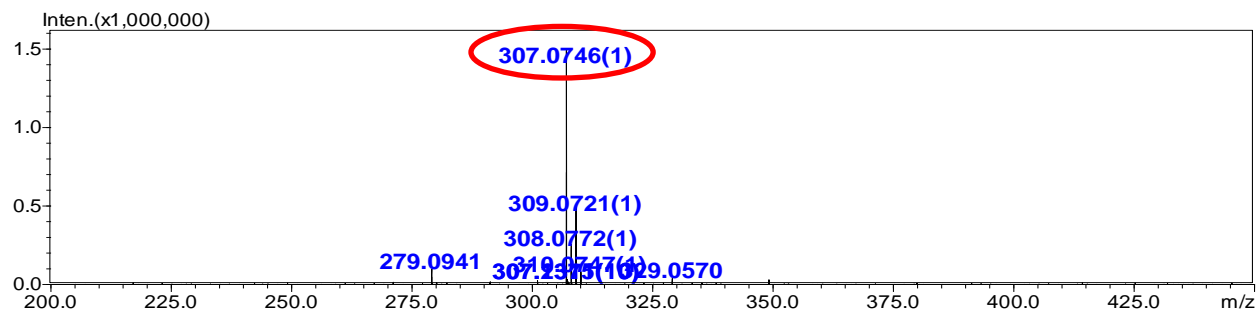


Figure S24. High-resolution mass spectra of **3**.

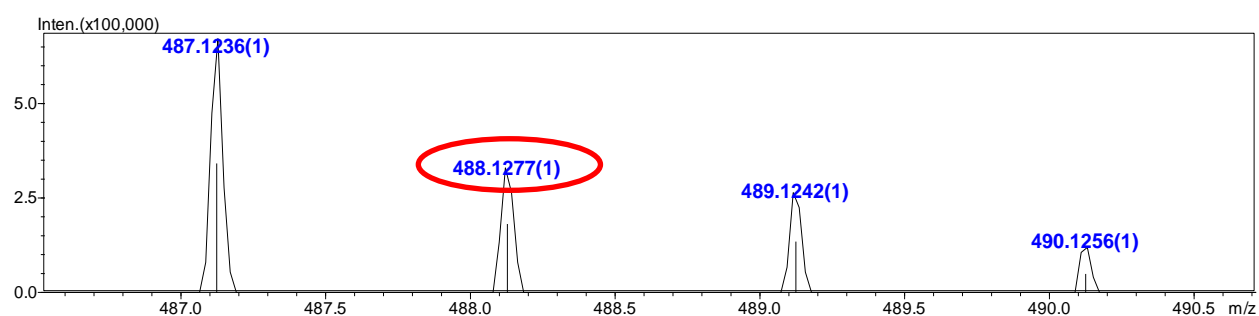


Figure S25. High-resolution mass spectra of **4**.

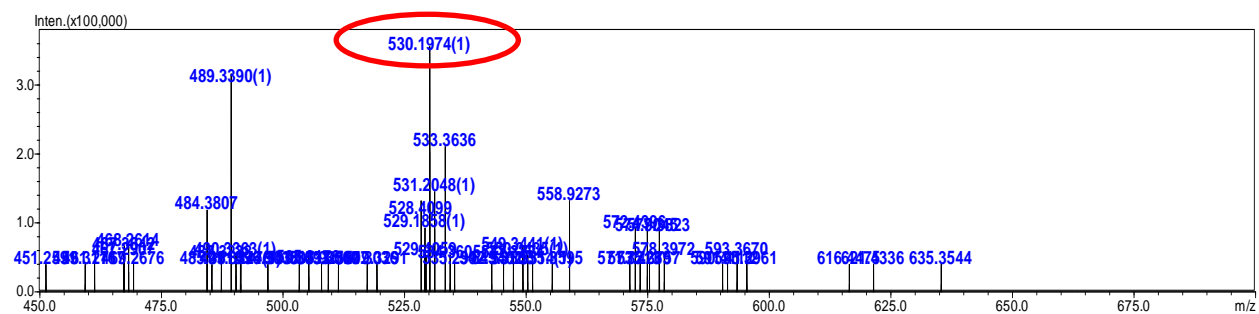


Figure S26. High-resolution mass spectra of **2-PXZ-PR**.

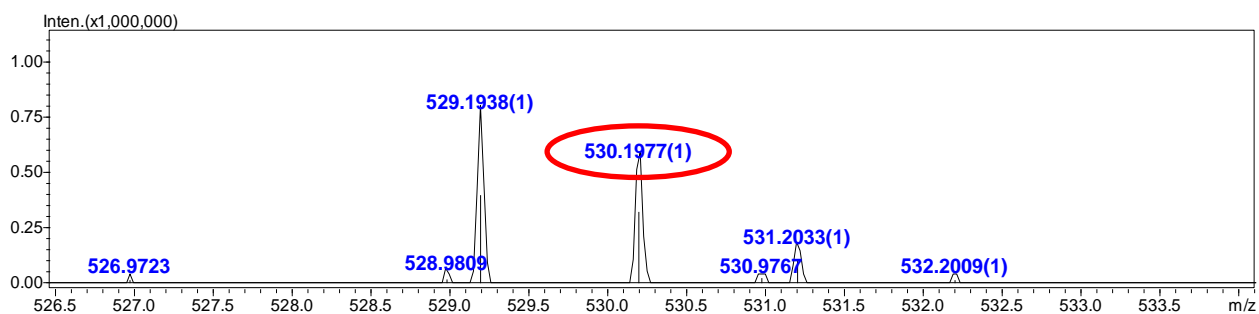


Figure S27. High-resolution mass spectra of **6-PXZ-PR**.

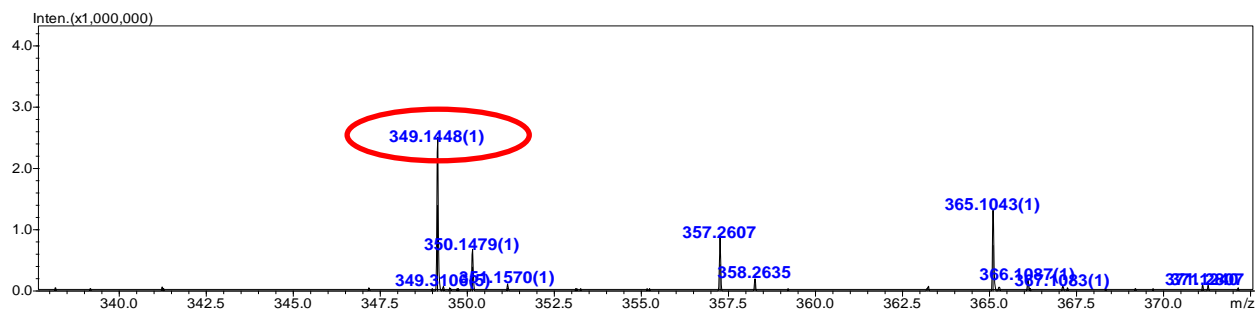


Figure S28. High-resolution mass spectra of **5**.

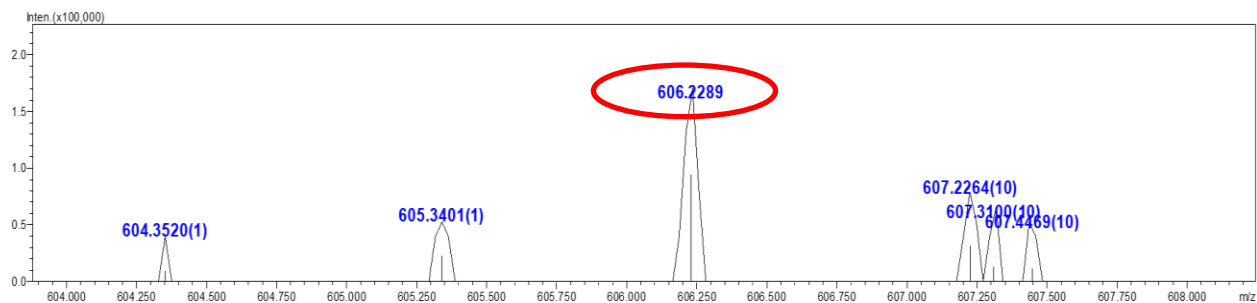


Figure S29. High-resolution mass spectra of **2-PXZ-PRB**.

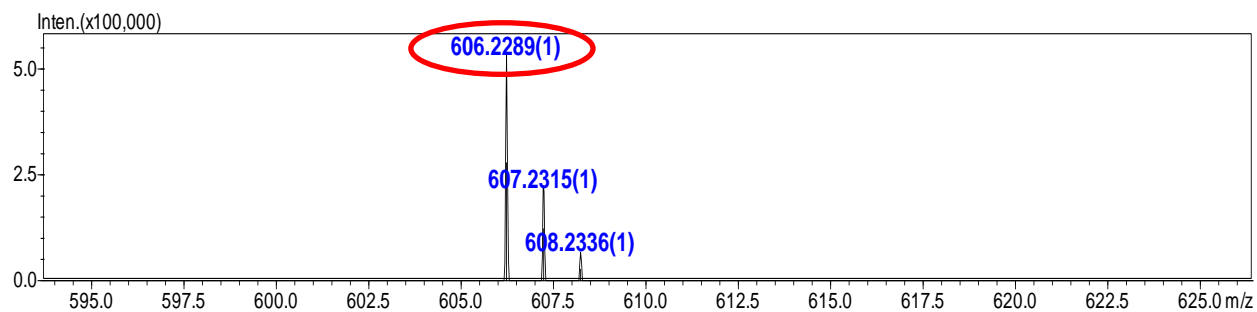


Figure S30. High-resolution mass spectra of **6-PXZ-PRB**.

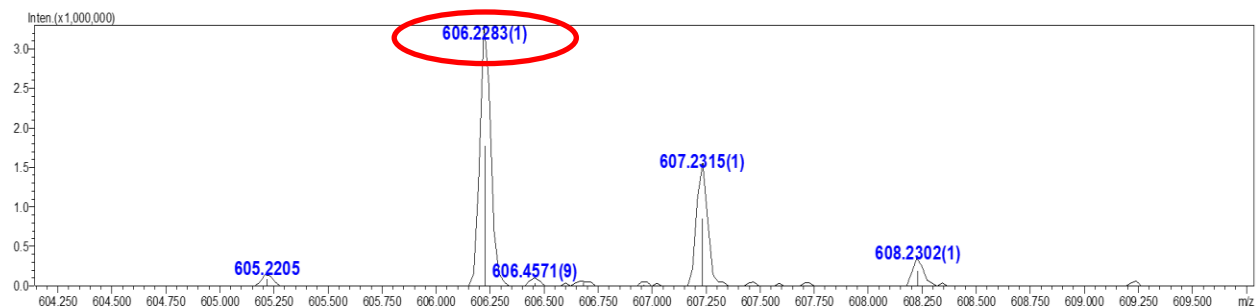


Figure S31. High-resolution mass spectra of **8-PXZ-PRB**.